Ferroelastic relaxation at 20 GHz evidenced by large frequency range picosecond acoustics

Arnaud Devos, F. Casset, G. Le Rhun, P. Emery, S. Fanget, E. Defay

Applied Physics Letters

Ferroelastic relaxation at 20 GHz evidenced by large frequency range picosecond acoustics

Cite as: Appl. Phys. Lett. **112**, 262905 (2018); https://doi.org/10.1063/1.5035479
Submitted: 16 April 2018 • Accepted: 09 June 2018 • Published Online: 27 June 2018

A. Devos, F. Casset, G. Le Rhun, et al.

Ferroelastic relaxation at 20 GHz evidenced by large frequency range picosecond acoustics

A. Devos,[1] F. Casset,[2] G. Le Rhun,[2] P. Emery,[3] S. Fanget,[2] and E. Defay[4]
[1]*Institut d'Electronique, de Microelectronique et de Nanotechnologie, Unite Mixte de Recherche CNRS 8250, Avenue Poincare, F-59652 Villeneuve d'Ascq, France*
[2]*CEA, LETI, MINATEC Campus, Grenoble 38054, France*
[3]*MENAPIC, Lille 59800, France*
[4]*Luxembourg Institute of Science and Technology, Department of Materials Research and Technology, 41 Rue du Brill, L-4422 Belvaux, Luxembourg*

(Received 16 April 2018; accepted 9 June 2018; published online 27 June 2018)

We present a method to perform elastic measurements on a thin-film as a function of frequency between a few GHz and a few hundred GHz. The technique is mainly based on Picosecond Acoustics (PA), which is an ultrafast optical technique that realizes pulse-echo measurements in the hypersonic range. Here, we combine gold layers serving as transducers and several opto-acoustic detection mechanisms to extend the PA technique to the lowest accessible frequencies (a few GHz) up to hundreds of GHz. We can therefore use the same technique on the same material to explore its elastic properties at a certain frequency over a very large frequency range. We have then applied this technique to explore the elastic properties of a lead zirconate titanate thin film from 3 to 80 GHz. We report a 9% increase in the longitudinal sound velocity above 20 GHz, which corresponds to a 19% increase in the C_{33} elastic modulus. We interpret such an observation as a direct evidence of ferroelastic domain wall relaxation. *Published by AIP Publishing.*
https://doi.org/10.1063/1.5035479

Picosecond acoustics (PA) has opened the door to high-resolution investigations of thin film elastic properties using non-destructive means.[1,2] Irradiation of an optically absorbing material with ultrashort optical pulses leads to the emission of acoustic waves with unprecedented high frequencies up to several hundreds of GHz.[3] For that, one takes advantage of the strong light absorption in metal (typically over a few nm) to excite a very small piece of matter from which a high frequency strain pulse results. Prior to such a discovery in the eighties, physical acoustics was limited to a few GHz, which is the maximum frequency that a conventional pulse echo technique can reach via transducers.

The PA technique gives us the opportunity to investigate elasticity in materials of reduced size. Can one expect similar results if elasticity is measured in the ultrasonic or hypersonic range? For most of the materials, the answer is yes, provided that one can certify that a thin film is chemically identical to its bulk form. This is, for example, the case of silica for which the same sound velocity has been measured from the Hz range up to several hundreds of GHz.[4]

It would be particularly interesting to explore the same question on a material experiencing an elasticity change in the GHz range. A few reports suggest that $SrTiO_3$ (STO) or lead zirconate titanate (PZT) could be a good candidate for such a change at high frequencies. Maerten *et al.* reported that GHz phonons can propagate and interact with ferroelastic domain walls (DWs).[5] They observed a strong softening in $SrTiO_3$ at 70 GHz at temperatures below its antiferrodistortive phase transition at 105 K. They deduced that the DW velocity should be on the order of the magnitude of sound velocity. It suggests that DW relaxation in STO should occur at frequencies above 70 GHz. About PZT, several authors have identified a large dielectric relaxation in bulk ceramics in this GHz range, such as Böttger and Arlt[6] and Buixaderas *et al.*[7] In PZT thin films, we observed via dielectric measurements that a clear ferroelectric relaxation takes place in PZT thin films between 10 and 40 GHz.[7,8] Schick *et al.* used femtosecond laser excitation combined with ultrafast x-ray diffraction experiments on epitaxial PZT thin films.[9] However, their set-up did not allow acoustic frequency control, which in turn infers that no acoustic velocity relaxation was detected.

The main idea of this work is to measure the sound velocity at various frequencies of a given thin film exhibiting a ferroelastic relaxation in the GHz range. The challenge is to be able to measure below and above the frequency at which the acoustic relaxation is expected to occur. PA provides a means of investigating the behavior of these materials over a large frequency range, though generating frequencies of just a few GHz is challenging. In this letter, we combine gold layers and several opto-acoustic detection mechanisms to extend the PA technique to the lowest accessible frequencies (a few GHz) up to hundreds of GHz enabling the exploration of elastic properties over a very large frequency range. We have then applied such a technique to a morphotropic PZT thin film from 3 to 80 GHz and evidenced a clear relaxation of PZT ferroelastic domain walls.

In PA, the frequency of the acoustic pulse is governed by the length over which the laser light is absorbed. However, the laser light is first absorbed by electrons before the energy is transferred to phonons less than 1 ps later. During this very short time-delay, the electrons can move over a distance larger than the optical absorption length, a distance that can be as large as the film thickness itself. In such a case, the acoustic pulses resulting from light absorption can be longer than expected. This is specifically the case of noble metals such as gold.[10,11]

This is beneficial for our present goal since we can control the central frequency of the acoustic pulse by adding on top of the sample a gold layer whose thickness is chosen to explore acoustic propagation at various frequencies. From the same PZT sample, we thus prepared a series of samples which only differ from the thickness of the top gold layer. As laser light is absorbed in the whole gold layer, the larger the layer, the lower the emitted acoustic frequency. Quantitatively, the central frequency f of the emitted pulse is given by the following equation:

$$f = \frac{C_{gold}}{2d}, \tag{1}$$

where d is the thickness of the gold film and c_{gold} is the longitudinal gold sound velocity ($c_{gold} = 3400$ m/s). Using a very thin gold layer (typically 15 nm) allows high frequencies in the 100 GHz range to be reached. On the contrary, a 280 nm thick gold film enables measurements around 6 GHz.

Regarding the detection in PA, the returning echo is optically detected through the photo-elastic mechanism. But, this mechanism is particularly inefficient in gold and furthermore not efficient for detecting low frequencies. To overcome such difficulties, we use an interferometric detection of the probe following the pioneering work of B. Perrin.[14] The optical response of the sample is probed using two beams instead of one, the first one seeing the sample before the generation and the second one reaching the same place after the generation of the acoustic pulse at various time-delays. The interferences between both beams enable a way to detect the sample surface displacement from which low frequency (LF) acoustic pulses can be easily detected. In the following, we apply this low frequency (LF) scheme to a gold layer whose thickness is in the 50–500 nm range.

For a thinner gold layer and to detect the higher part of the acoustic spectrum, we introduce the High-Frequency (HF) regime that corresponds to a gold layer thickness between 0 and 20 nm. In such a case, the gold layer is semi-transparent and the propagation of the acoustic pulse in the PZT layer can be followed by detecting acousto-optic oscillations.[16] When a pulse propagates in PZT, light and sound interact within the transparent layer and an oscillation is detected in the time-domain. A specific frequency f of the acoustic pulse is detected as

$$f = \frac{2nc_L}{\lambda}, \tag{2}$$

where n is the PZT optical index, c_L the PZT longitudinal sound velocity and λ the probe wavelength. In the blue range, one can reach the 50–80 GHz acoustic frequency range.

A sol-gel PZT thin film was deposited on an 8 inch silicon wafer. First, oxidation of the substrate surface was performed (500 nm thick) and a 100 nm thick Pt bottom electrode was sputtered. Then, a (100)-oriented 506 nm thick sol-gel PZT was deposited. The Zr/Ti ratio in at. % is set to 52/48. After spinning, each single PZT sol-gel layer was baked at 120 °C for 30 s on a hot plate to evaporate its solvents and then heated up to 350 °C for 5 min in air to suppress all organic components of the initial sol. The process was repeated three times. PZT crystallization is then provided through Rapid Thermal Annealing (RTA) performed at 700 °C in air for 30 s. The whole procedure was carried out three times until the desired PZT thickness had been obtained.[17] The wafer with the PZT layer was then cut to obtain $1 \times 1\,\text{cm}^2$ samples, which ensures PZT thickness uniformity. Finally, gold transducers were evaporated with thicknesses from 15 to 630 nm. From Eq. (1), we calculated that the expected frequencies theoretically span from 2.7 GHz to 80 GHz. Table I summarizes the studied samples, their operating regime (LF or HF), the expected acoustic frequency and the detection mechanism.

The time-resolved measurements were performed using a two-color pump and probe setup associated with a tunable Ti:Sapphire oscillator. The laser produces 120 fs optical pulses at a repetition rate of 80 MHz centered at a wavelength tunable between 690 and 1050 nm with energy in the nano-joule range. Two-color measurements were performed by combining a beam directly derived from the oscillator and another which is frequency doubled. The probe beam is time-delayed with respect to the pump. Beams are focused at the sample surface at normal incidence and with a spot of 20 μm in diameter. Two configurations are used for the probe detection. In transient reflectometry, the reflected probe intensity is monitored as a function of the time-delay between the pump and the probe. In transient interferometry, the probe beam is divided into two parts that reach the sample following long and short arms of a common path interferometer. One probe reaches the sample always before the pump, whereas the second does so at a variable delay. Both beams follow reverse paths and finally interfere in two detectors. From such interferences, the low frequency surface displacement can be detected as the returning echo reaches the gold layer. More details and a schematic view of the setup can be found in Ref. 15.

We first present measurements in the HF regime on sample 0 reproduced in Fig. 1(a). The transient reflectivity is measured on a bare PZT sample (no metal on top) using an infrared pump (centered at 900 nm) and a blue probe (450 nm). At $t = 0$, both the pump and the probe laser reach the sample simultaneously. A sharp peak is detected and it results from the photo-excitation of the electrons in the buried Pt layer. The energy first captured by electrons is rapidly transferred to phonons and an acoustic pulse is emitted from the Pt layer. One part is transmitted to the PZT layer and we observe an oscillation related to acousto-optic interactions in PZT. As shown in the schematic view of Fig. 1(b), the probe

TABLE I. Samples and acoustic frequencies according to gold thickness deposited on top of the PZT film. HF and LF, respectively, designate High and Low Frequency.

Sample	Operating regime	Gold thickness (nm)	Acoustic frequency (GHz)	Detection
0	HF	0	50–80	Brillouin
1	HF	15	50–80	Brillouin
2	LF	80	21.3	Interferometry
3	LF	250	6.8	Interferometry
4	LF	280	6.1	Interferometry
5	LF	630	2.7	Interferometry

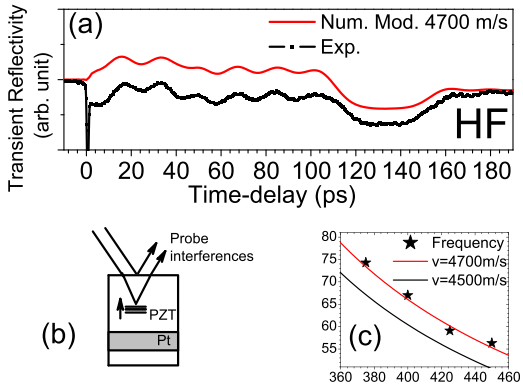

FIG. 1. (a) Transient reflectivity as measured on sample 0. The acousto-optic oscillation and the reflectivity step detected near 120 ps are both reproduced very well with a numerical model assuming a sound velocity of 4700 m/s in PZT. (b) Schematic view of the acousto-optic detection in PZT. (c) Dependence of the Brillouin frequency on the probe wavelength. Dots are the measured frequencies and continuous lines have been obtained via Eq. (2) for two values of PZT sound velocity.

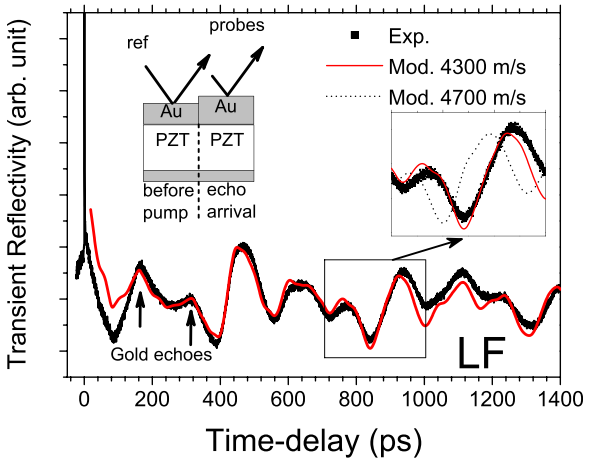

FIG. 2. PA signal measured on the 280 nm thick gold transducer sample compared with simulation. The acoustic frequency here is 6.1 GHz, corresponding to the LF regime. Inset: the signal between 700 and 1000 ps, compared to a numerical model using a PZT acoustic velocity of 4300 or 4700 m/s.

laser light penetrates the transparent PZT layer and several reflections of the probe interfere, which infers a Brillouin oscillation in the time domain. By measuring the frequency of such an oscillation, we can extract the sound velocity in PZT using Eq. (2).

To observe such an oscillation, the acoustic pulse must contain the Brillouin frequency. Thus, we have a high frequency emission from the Pt electrode. On sample 1, the top Au film is thin enough to let a part of the probe beam penetrate the PZT layer and the same Brillouin oscillation is detected.

Similar measurements have been performed at various laser wavelengths. The detected frequency shows a strong dependence on the probe wavelength as expected. In Fig. 1(c), the experimental data are compared to a model based on Eq. (2), in which we introduced the optical dispersion in PZT. The excellent agreement between the model and the experimental data first confirms the interpretation of an acousto-optic interaction detected in PZT. This also shows that the PZT sound velocity is close to 4700 m/s in the 50–80 GHz frequency range.

In Fig. 1(a), the signal near 120 ps presents a step in the transient reflectivity.[16] Such a contribution is detected when the acoustic pulse emitted from the Pt layer is reflected by the free surface. The sound velocity can be alternatively deduced from the step delay and the film thickness. To further understand the origin of the signal, numerical simulations were performed according to the theories of acoustic generation, propagation and detection, as previously elaborated by others.[12,13] As shown in Fig. 1(a), the numerical model reproduces very well the whole time-domain response, assuming a sound velocity of 4700 m/s. Other contributions visible near 40 ps and 150 ps are related to the pulse emitted towards the substrate and mostly reflected at the Pt/SiO_2 interface.

On samples 0 and 1, HF measurements have been performed. An acousto-optic oscillation is observed whose period fits perfectly the model assuming a PZT sound velocity of 4700 m/s. On sample 0, this value is independently confirmed from the PZT thin film thickness and the delay at which a reflectivity step is observed.

We now examine the results obtained in the LF regime on samples 2–5. Figure 2 shows the PA interferometric signal obtained on sample 3 that is covered with a 280 nm-thick gold layer. After the sharp peak detected at zero delay, an acoustic pulse is generated in gold and propagates towards the substrate. The pulse is partially reflected at the interface between gold and PZT so that a part of the initial strain pulse remains confined within the gold layer. When this pulse is reflected at the free surface, the surface displacement is detected as large echoes, visible near 160 and 320 ps in Fig. 2. Damping of such a contribution is related to both transmission into the PZT layer and acoustic damping in gold. The measurement of the time delay between such echoes allows us to calculate the central frequency at which the measurement has been made. On sample 3, we measured a time-of-flight of 164 ps, which leads to a frequency of 6.1 GHz, in good agreement with the expected frequency.

A second set of echoes then appears around 400 ps (Fig. 2). They are issued from the round trip of the initial acoustic pulse through the gold/PZT bi-layer. This is supported by the detection of a series of replica echoes in the gold layer after the first echo was separated by the same delay as in the first series of echoes. A second round-trip in the gold/PZT bi-layer is observed after 800 ps.

Clearly, the measured signal is composed of the superposition of several series of echoes issued from multiple reflections at various interfaces. To gain further understanding, we compared experimental data to simulation. The numerical model implements the photo-acoustic generation in the gold layer and the optical detection of the surface displacement. The main data needed as inputs of the model are the optical index and the sound velocity of the materials, and thickness of the successive layers. As shown in Fig. 2, the agreement between both signals is excellent, over a very large time delay window.

An important conclusion is that we need to use a lower value for the sound velocity in PZT in the LF experiment (4300 m/s) compared to HF measurements (4700 m/s) to obtain such a good agreement. As shown in the inset of Fig. 2, the second set of echoes issued from PZT cannot be

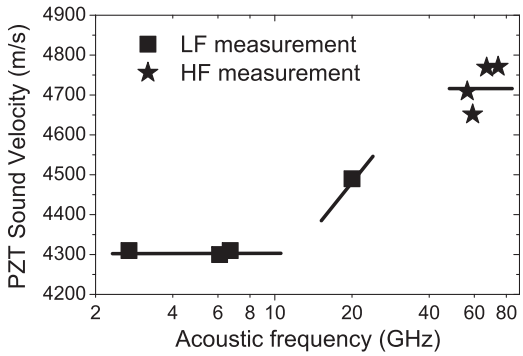

FIG. 3. Compilation between the PZT longitudinal sound velocities measured at frequencies from 3 to 80 GHz. LF and HF refer to the technique used to measure sound velocity as explained in Table I.

reproduced using the HF velocity value. Similar measurements and data extractions were performed on samples 2–5. For each sample, the acoustic frequency at which the measurement was made was obtained from the time-of-flight in gold. The PZT sound velocity was obtained through a numerical fit of the measured signal.

LF signals cannot be reproduced using a 4700 m/s sound velocity in PZT (inset Fig. 2), and conversely, HF results cannot be fitted using 4300 m/s as shown in Fig. 1(c) where the expected results for 4500 m/s are already far from measured data. Figure 3 displays the longitudinal acoustic velocities as a function of acoustic frequency for all the investigated samples, all of them being issued from the same PZT thin film. We compile the data obtained in the LF regime using various gold transducer thicknesses and data from HF measurements performed at various laser-wavelengths. It first reveals that the PZT sound velocity is clearly different below 10 GHz and above 40 GHz with the relaxation frequency occurring around 20 GHz. The PZT longitudinal acoustic velocity appears to be 9% higher above 50 GHz rather than below 10 GHz. Such an increase corresponds to a 19% increase in the longitudinal elastic modulus C_{33}.

Such a significant increase in the elastic modulus is likely to be related to a ferroelastic DW relaxation. Indeed, DW movements soften materials. Beyond the relaxation frequency, DWs are not mobile anymore, so that the PZT stiffness, and thus the acoustic velocity, increases. Note that we are specifically dealing with ferroelastic domains, which correspond to ferroelectric non-180° domains in PZT. There are other experimental evidence supporting the idea of DW relaxation in the GHz range notably in bulk ceramics.[6,7] Besides, one of the authors reported ferroelectric DW relaxation in PZT thin films deposited on glass substrates.[17] This relaxation was taking place around 10 GHz through the steep decrease in the PZT dielectric constant together with a strong increase in its dielectric losses as one would expect from a typical Debye relaxation behavior. As we consider similar PZT thin films, it seems logical to associate the ferroelastic relaxation with the ferroelectric one. Indeed, in PZT, all ferroelastic domains are also ferroelectric. The increase in the relaxation frequency of these thin films (∼20 GHz) compared to the bulk (∼1 GHz) is likely linked with the size of the domains and DWs, as suggested by Böttger and Arlt.[6] Knowing the upper limit of such a relaxation could trigger ideas for applications above 50 GHz (phase shifter for radars at 77 GHz, for instance), since the losses should be significantly reduced.

In conclusion, we have presented a way of using the PA technique to probe the elastic properties of thin films as a function of frequency. Gold transducers have been used to control the central emission frequency in the LF regime. Combined with an interferometric detection, frequencies as low as a few GHz have been detected. Conversely, the tunability of the laser has been used to select a specific frequency in the HF range typically greater than 50 GHz. We have then applied such a scheme to a PZT thin film and measured its sound velocity from 3 to 80 GHz. We report a 9% increase in the longitudinal sound velocity above 20 GHz, which is interpreted as a direct observation of the ferroelastic domain wall relaxation. Higher frequencies than those presented in this paper could be reached using the same scheme: for example, Brillouin oscillations used in this work for the HF measurement can reach more than 120 GHz in AlN[18] and more than 300 GHz in Si.[19] Such a modified PA technique could thus be used as a generic characterization means to identify phase transitions in the whole GHz range.

The authors would like to thank Dr. A. Le Louarn and Dr. S. Sadtler for their precious assistance during measurements. E.D. would like to thank the Luxembourg National Research Fund for supporting this study via Grant No. CoFermat FNR/P12/4853155/Kreisel. Moreover, we are indebted to M. Guennou, C. Cochard, and T. Granzow for fruitful discussions.

[1]C. Thomsen, J. Strait, Z. Vardeny, H. J. Maris, J. Tauc, and J. J. Hauser, Phys. Rev. Lett. **53**, 989 (1984).
[2]A. Devos, Ultrasonics **56**, 90 (2015).
[3]P.-A. Mante, A. Devos, and A. Le Louarn, Phys. Rev. B **81**, 113305 (2010).
[4]S. Ayrinhac, M. Foret, A. Devos, B. Rufflé, E. Courtens, and R. Vacher, Phys. Rev. B **83**, 014204 (2011).
[5]L. Maerten, A. Bojahr, M. Gohlke, M. Rössle, and M. Bargheer, Phys. Rev. Lett. **114**, 047401 (2015).
[6]U. Böttger and G. Arlt, Ferroelectrics **127**, 95 (1992).
[7]E. Buixaderas, D. Nuzhnyy, P. Vaněk, I. Gregora, J. Petzelt, V. Porokhonskyy, L. Jin, and D. Damjanović, Phase Transitions **83**, 917 (2010).
[8]E. Defay, T. Lacrevaz, T. T. Vo, V. Sbrugnera, C. Bermond, M. Aid, and B. Flechet, Appl. Phys. Lett. **94**, 052901 (2009).
[9]D. Schick, A. Bojahr, M. Herzog, P. Gaal, I. Vrejoiu, and M. Bargheer, Phys. Rev. Lett. **110**, 095502 (2013).
[10]G. Tas and H. J. Maris, Phys. Rev. B **49**(21), 15046 (1994).
[11]O. B. Wright, Phys. Rev. B **49**, 9985 (1994).
[12]C. Thomsen, H. T. Grahn, H. J. Maris, and J. Tauc, Phys. Rev. B **34**, 4129 (1986).
[13]O. B. Wright and T. Hyoguchi, Opt. Lett. **16**, 1529 (1991).
[14]B. Perrin, C. Rossignol, B. Bonello, and J.-C. Jeannet, Physica B **263–264**, 571 (1999).
[15]A. Devos, S. Sadtler, P.-A. Mante, A. Le Louarn, and P. Emery, Appl. Phys. Lett. **105**, 231905 (2014).
[16]A. Devos, J.-F. Robillard, R. Côte, and P. Emery, Phys. Rev. B **74**(6), 064114 (2006).
[17]M. Cueff, E. Defay, P. Rey, G. Le Rhun, F. Perruchot, C. Ferrandon, D. Mercier, F. Domingue, A. Suhm, M. Aid, L. Liu, S. Pacheco, and M. Miller, in *2010 IEEE 23rd International Conference on Micro Electro Mechanical Systems (MEMS)* (2010), p. 212.
[18]A. Devos, R. Côte, G. Caruyer, and A. Lefebvre, Appl. Phys. Lett. **86**(21), 211903 (2005).
[19]J. Costa Dantas Faria, P. Garnier, and A. Devos, Appl. Phys. Lett. **111**, 243105 (2017).